

Voltage-dependent inactivation gating at the selectivity filter of the MthK K⁺ channel

Andrew S. Thomson and Brad S. Rothberg

Department of Biochemistry, Temple University School of Medicine, Philadelphia, PA 19140

Voltage-dependent K⁺ channels can undergo a gating process known as C-type inactivation, which involves entry into a nonconducting state through conformational changes near the channel's selectivity filter. C-type inactivation may involve movements of transmembrane voltage sensor domains, although the mechanisms underlying this form of inactivation may be heterogeneous and are often unclear. Here, we report on a form of voltage-dependent inactivation gating observed in MthK, a prokaryotic K⁺ channel that lacks a canonical voltage sensor and may thus provide a reduced system to inform on mechanism. In single-channel recordings, we observe that Po decreases with depolarization, with a half-maximal voltage of 96 ± 3 mV. This gating is kinetically distinct from blockade by internal Ca²⁺ or Ba²⁺, suggesting that it may arise from an intrinsic inactivation mechanism. Inactivation gating was shifted toward more positive voltages by increasing external [K⁺] (47 mV per 10-fold increase in [K⁺]), suggesting that K⁺ binding at the extracellular side of the channel stabilizes the open-conductive state. The open-conductive state was stabilized by other external cations, and selectivity of the stabilizing site followed the sequence: K⁺ \approx Rb⁺ > Cs⁺ > Na⁺ > Li⁺ \approx NMG⁺. Selectivity of the stabilizing site is weaker than that of sites that determine permeability of these ions, suggesting that the site may lie toward the external end of the MthK selectivity filter. We could describe MthK gating over a wide range of positive voltages and external [K⁺] using kinetic schemes in which the open-conductive state is stabilized by K⁺ binding to a site that is not deep within the electric field, with the voltage dependence of inactivation arising from both voltage-dependent K⁺ dissociation and transitions between nonconducting (inactivated) states. These results provide a quantitative working hypothesis for voltage-dependent, K⁺-sensitive inactivation gating, a property that may be common to other K⁺ channels.

INTRODUCTION

During sustained depolarization, many voltage-gated K⁺ channels (Kv channels) undergo C-type inactivation, resulting in a decay of the outward K⁺ current over the time scale of hundreds to thousands of milliseconds, and thus contributing to mechanisms of tuning of the cellular responses to electrical excitation (Hoshi et al., 1991; Yellen, 1998; Hille, 2001). In the HERG (Kv11.1) channel, the time course of C-type inactivation is more rapid than that of channel opening, resulting in apparent inward rectification in these channels (Smith et al., 1996). This mechanism is critical in the pacing of cardiac action potentials, and mutations in HERG that attenuate inactivation can lead to cardiac arrhythmia and sudden death (Brugada et al., 2004; Cordeiro et al., 2005; McPate et al., 2005).

The kinetics of C-type inactivation in K⁺ channels are sensitive to extracellular concentrations of permeant ions and the K⁺ channel blocker TEA⁺ (Grissmer and Cahalan, 1989; Choi et al., 1991; Baukowitz and Yellen, 1995), as well as mutations and site-specific chemical modification of side chains near the extracellular end of the K⁺ channel selectivity filter (Hoshi et al., 1991; López-Barneo et al., 1993; Yellen et al., 1994; Liu et al., 1996), consistent with the idea that C-type inactivation

is the result of a conformational change at or near the selectivity filter. Interestingly, fluorescent labeling of residues in the voltage sensor domains of Kv channels can also track the time course of C-type inactivation, suggesting that C-type inactivation may involve energetic and/or physical coupling between movements of the voltage sensor and pore domains (Loots and Isacoff, 2000; Smith and Yellen, 2002). However, it is not clear whether this coupling is obligatory, especially in light of inactivation gating that occurs in KcsA, a prokaryotic K⁺ channel that lacks a canonical voltage sensor domain (Cordero-Morales et al., 2006, 2007).

Here, we report on a form of inactivation that occurs in MthK, a prokaryotic channel that lacks a canonical voltage sensor. We observe that inactivation in MthK shares properties with C-type inactivation in Kv channels, most notably sensitivity to [K⁺] and other ions at the external side of the channel. In recordings of single MthK channels incorporated into planar lipid bilayers, we observe that in symmetrical 200-mM KCl solutions, depolarization decreased open probability (Po) with a half-maximal voltage of 96 ± 3 mV. Po did not increase

Correspondence to Brad S. Rothberg; rothberg@temple.edu

substantially by decreasing internal $[Ca^{2+}]$, suggesting that this process does not result solely from Ca^{2+} blockade, and the kinetics of voltage-dependent closings were distinct from Ba^{2+} blockade. Collectively, these observations suggest that this gating phenomenon is not from slow ionic blockade, but may involve intrinsic inactivation. MthK inactivation was inhibited by increasing external K^+ and other cations, following the selectivity sequence of $K^+ \approx Rb^+ > Cs^+ > Na^+ > Li^+ \approx NMG^+$, consistent with MthK inactivation being sensitive to occupancy of at least one moderately K^+ -selective site in the pore. We could describe MthK Po over a wide range of voltage and external $[K^+]$ with a kinetic scheme in which the open-conductive conformation is stabilized by K^+ binding. These results provide a working hypothesis for voltage-dependent, K^+ -sensitive inactivation gating—a property that may be common to other K^+ channels—and a quantitative framework for understanding the ionic mechanisms underlying inactivation in these channels.

MATERIALS AND METHODS

Channel purification and reconstitution

MthK was expressed, purified, and reconstituted into proteoliposomes, as described previously (Parfenova et al., 2006; Pau et al., 2010). Channels were reconstituted into liposomes composed of *Escherichia coli* lipids (Avanti Polar Lipids, Inc.) and rapidly frozen in liquid N_2 and stored at $-80^\circ C$ until use. Protein concentrations in liposomes ranged from 10 to 50 μg of protein per milligram of lipid.

Lipid bilayer recording and solution changes

Recordings were obtained using planar lipid bilayers of POPE/POPG (3:1) in a horizontal bilayer chamber at $22-24^\circ C$, as described previously (Pau et al., 2010). For experiments involving the changing of salt solutions at the cytoplasmic side of the channel, solution in the cis (top) chamber contained 200 mM KCl and 10 mM HEPES, pH 7.0, with no added Ca^{2+} (to suppress the activity of MthK channels that were incorporated with their cytoplasmic face toward the cis chamber). Solutions in the trans (bottom) chamber contained 200 mM KCl and 10 mM HEPES, with $CaCl_2$ and other salts added to reach the indicated concentrations, at pH 7.3. Because we typically used high Ca^{2+} (5–10 mM) to fully activate the channels, Ca^{2+} buffers were not used in the recording solutions. The adjustment of pH for these 200-mM KCl solutions required 0.2–0.25 ml of a 1-M KOH stock solution, resulting in a nominal further increase in $[K^+]$ (≤ 1 mM).

For experiments involving the changing of salt solutions at the external side of the channel, solution in the cis (top) chamber contained 200 mM KCl, 10 mM HEPES, and 10 mM $CaCl_2$, pH 7.3 (pH adjustment by KOH increased the final $[K^+]$ by ≤ 1 mM). Solution in the trans (bottom) chamber contained 0–800 mM KCl and 10 mM HEPES, pH 7.0. For the 800-mM KCl solution, pH adjustment by KOH increased the final $[K^+]$ by ~ 3 mM. In experiments where $[KCl]$ was < 200 mM, KCl was replaced by NMG to maintain osmolarity; for these solutions, pH was adjusted using HCl, which would not be expected to change the final $[K^+]$. In experiments where KCl was substituted with 200 mM RbCl, CsCl, NaCl, or LiCl, pH was adjusted to 7.0 using the hydroxide salts of these cations, which may have resulted in nominal increases in concentrations of the respective cations (~ 1 mM).

Within each bilayer, multiple solution changes were performed using a gravity-fed perfusion system, as described previously (Pau

et al., 2010). To ensure completeness of solution changes, the trans chamber was washed with a minimum of 15 ml (~ 15 chamber volumes) of solution before recording under a given set of conditions.

Electrophysiological data analysis

Single-channel currents were amplified using a patch clamp amplifier (PC-ONE; Dagan Corporation), with low-pass filtering to give a final effective filtering of 333 Hz (dead time of 0.538 ms), and sampled by computer at a rate of 50 kHz. Currents were analyzed by measuring durations of channel openings and closings at each current level by 50% threshold analysis using pClamp 9.2 (MDS Analytical Technologies). These were used to calculate NPo as:

$$NPo = \sum_{i=1}^n iP_i, \quad (1)$$

where i is the open level and P_i is the probability of opening at that level. The mean single-channel Po is obtained by dividing NPo by N, which is the number of channels in the bilayer, determined by recording under conditions where the maximum level of channel opening can be observed. The voltage dependence of Po was described by the Boltzmann equation,

$$Po = Pomax / (1 + \exp(z\delta(V - V_{1/2}) / k_B T)), \quad (2)$$

where Pomax is the maximal Po, $z\delta$ is the effective gating valence (in e_0), $V_{1/2}$ is the voltage at half-maximal Po, k_B is Boltzmann's constant, and T is temperature. For data where Po at a given voltage was described as a function of external $[K^+]$ ($[K^+]_{ext}$), data were fitted with a form of the Hill equation,

$$Po = Pomax / \left(1 + \left([K^+]_{ext} / EC_{50} \right)^{n_H} \right), \quad (3)$$

where EC_{50} is the $[K^+]_{ext}$ required to reach half-maximal Po, and n_H is the fitted Hill coefficient.

Data points (e.g., Po and mean interval durations) are presented as mean \pm SEM of three to five independent observations for each data point and collectively represent data from a total of 20 different bilayers.

Correction of mean interval durations for missed events

The limited time resolution of the bilayer recording system can lead to distortion of open and closed event durations (Magleby and Weiss, 1990; Magleby, 1992). Specifically, under conditions where the mean observed opening duration is close to the system dead time, it is predicted that a significant fraction of openings will go undetected, resulting in artificial lengthening of closed intervals (and vice versa). To reduce the contribution of these effects to our analysis of MthK inactivation kinetics, we applied a simple correction to mean open and closed times (Blatz and Magleby, 1986). Correction of closed times was applied using:

$$c_{corr} = c_{obs} \times \exp\left[-(o_{obs} - t_{dead}) / t_{dead}\right] - t_{dead}, \quad (4)$$

where c_{corr} is the corrected mean closed time, c_{obs} is the observed mean closed time, o_{obs} is the observed mean open time, and t_{dead} is the system dead time. Correction of open times was applied with the same equation, except with “open” substituted for “closed” and vice versa. The correction factor applied to mean closed times was sometimes substantial, up to 42% (see Fig. 1 D), and thus prevented potentially erroneous interpretation of kinetic data. Mean interval duration ($A(V)$) was described as a function of voltage by:

$$A(V) = A(0)\exp(z\delta V / k_B T), \quad (5)$$

where $A(0)$ is the mean interval duration extrapolated to 0 mV.

Kinetic modeling

MthK gating was analyzed further by global fitting of P_o data as a function of $[K^+]$ and voltage within the framework of several candidate gating schemes. Rate constants for each kinetic scheme were constrained by the observed 2-D dwell-time distributions of adjacent open and closed intervals (Rothberg et al., 1997; Rothberg and Magleby, 1998, 1999, 2000). In brief, adjacent open- and closed-interval durations at each voltage and $[K^+]$ were log-binned to generate 2-D dwell-time distributions. For a given scheme, a set of initial rate constants was used to predict a given set of 2-D dwell-time distributions (i.e., over a range of voltage and $[K^+]$). These were each compared statistically (by log-likelihood values) to the observed 2-D dwell-time distributions obtained under the same conditions. The rate constants in the scheme and their voltage dependences were then changed, one at a time, to maximize the likelihood of the predicted dwell-time distributions, until additional changes yielded no increase in likelihood (an upper limit of $25,000 \text{ s}^{-1}$ was placed on each effective rate during the fitting). Schemes were refitted several times using different starting parameters to ensure that the most likely rate constants were found. Rates of

K^+ -dependent transitions were determined by multiplying second-order rate constants by $[K^+]$.

Because of higher ionic strength, the estimated K^+ activity coefficient is slightly lower for the 800-mM KCl solution in our experiments than solutions containing $\leq 200 \text{ mM}$ KCl. To account for a possible effect of ionic strength in our kinetic modeling that would result in a lower K^+ activity coefficient, we also fitted schemes using an effective $[K^+]$ of 688.8 mM in place of 800 mM. This was based on K^+ activity coefficients of 0.618 for 800 mM KCl and 0.718 for 200 mM KCl (Kaye and Laby, 1995); $(0.618/0.718) \times 800 \text{ mM} = 688.8 \text{ mM}$. Because the ionic strengths in solutions containing $< 200 \text{ mM}$ KCl were kept constant by the addition of NMG, we assumed that K^+ activity for these solutions did not vary much over $[KCl]$ ranging from 2 to 200 mM.

Kinetic schemes were ranked based on the Schwarz criterion (SC),

$$SC = -L + (0.5F)(\ln N), \quad (6)$$

where L is the log-likelihood, F is the number of free parameters, and N is the number of fitted open-closed pairs (Schwarz, 1978;

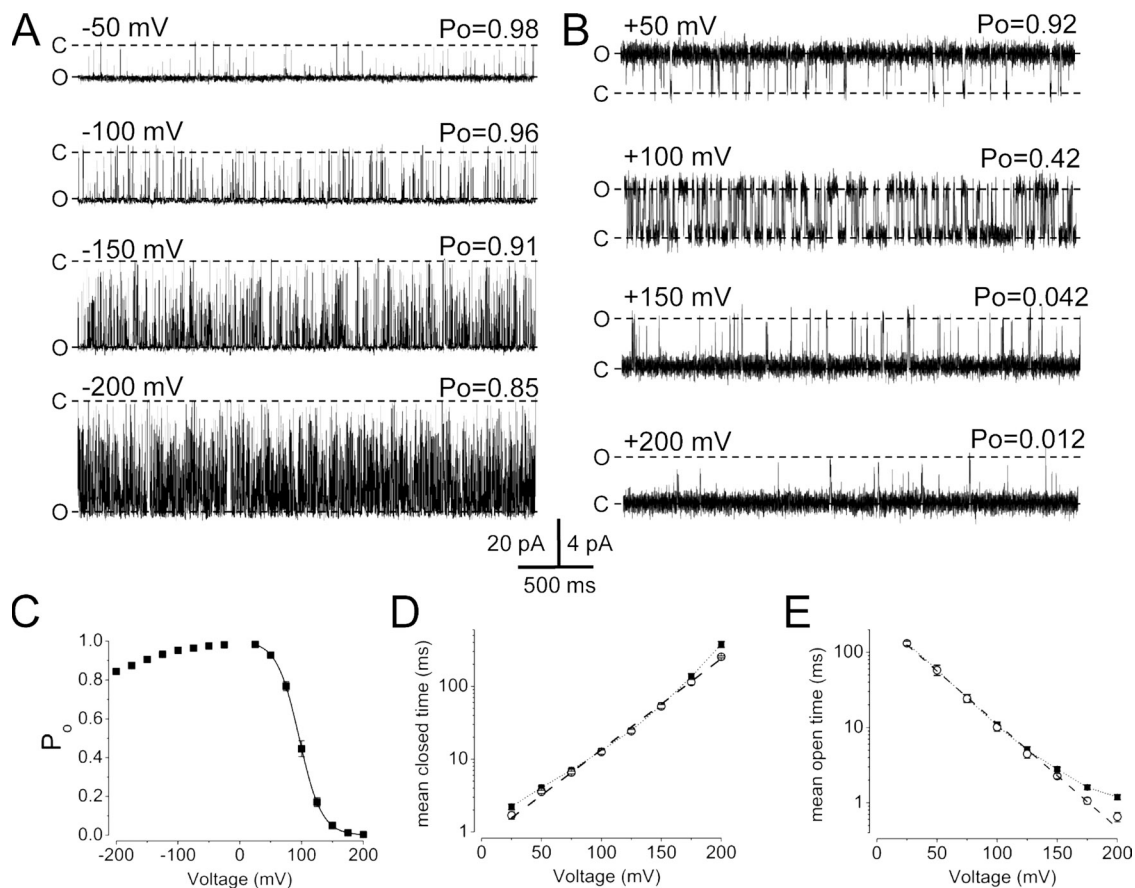


Figure 1. Voltage-dependent gating of MthK. (A) Representative inward current through a single MthK channel in symmetrical 200 mM KCl, with 20 mM Ca^{2+} at the cytoplasmic side of the channel. At negative voltages, P_o decreases slightly with increasing hyperpolarization because of the increased frequency of brief (flicker) closings, as described previously (Zadek and Nimigean, 2006). (B) Outward current through the same MthK channel under the same ionic conditions. P_o decreases strongly with increasing depolarization because of increases in both the duration and frequency of closings. (C) Mean P_o versus voltage. At positive voltages, the P_o versus voltage relation is described by a single Boltzmann equation (solid line; refer to Materials and methods) with a $V_{1/2}$ of 96 mV and gating valence ($z\delta$) of $1.4 e_0$. (D) Raw mean closed times (filled squares) deviated slightly from a simple exponential voltage dependence, but were fitted well by a single exponential after the application of a correction for missed events (open circles, corrected data; dashed line, exponential fit). (E) Likewise, mean open times (filled squares) deviated from a simple exponential voltage dependence, but this too could be accounted for after correction for missed events (open circles, corrected data; dashed line, exponential fit).

McManus and Magleby, 1991; Rothberg and Magleby, 1998). By this criterion, the scheme with the lowest SC is the top-ranked scheme.

Online supplemental material

Fig. S1 depicts kinetic Schemes 2–6, which were developed to test alternative hypotheses of the $[K^+]_{ext}$ and voltage dependence of MthK gating at depolarized voltages. Fig. S2 shows the mean open and closed times predicted from Schemes 1 and 6, with the most likely rate constants for “Channel 1” (see Table I) superimposed on the experimental data. Table S1 presents the statistical ranking of Schemes 1–6, and Table S2 presents the most likely rate constants for Scheme 6, constrained by kinetic data from three different representative MthK channels. The online supplemental material is available at <http://www.jgp.org/cgi/content/full/jgp.201010507/DC1>.

RESULTS

MthK channels close with depolarization

MthK gating is activated by Ca^{2+} and inhibited by H^+ , with both ligands acting at the cytoplasmic side of the channel. The mechanism underlying gating by these ligands can be described by an allosteric model in which eight Ca^{2+} bind to the cytoplasmic side of the channel to energetically stabilize the open state, while eight H^+ inhibit opening by destabilizing the Ca^{2+} -bound states (Zadek and Nimigean, 2006; Pau et al., 2010).

Despite the lack of a canonical voltage sensor domain, MthK is also gated by voltage (Zadek and Nimigean, 2006). In symmetrical 200-mM KCl solutions with 10 mM Ca^{2+} at the cytoplasmic side of the channel, we have observed a biphasic voltage dependence of P_o , consistent with

two voltage-dependent processes (Fig. 1). At negative voltages (from -200 to 0 mV), P_o increases weakly with depolarization from ~ 0.85 to 0.97 , largely because of a decrease in the frequency of brief flicker closings (Fig. 1, A and C). At positive voltages, however, P_o decreases, with a stronger voltage dependence than that observed at negative voltages (Fig. 1, B and C). With symmetrical 200 mM KCl, the relation between P_o and voltage was described by a Boltzmann equation with an apparent gating valence of $1.4 \pm 0.006 e_0$ and $V_{1/2}$ of 96 ± 3 mV. Because MthK channels do not contain a canonical voltage sensor domain, the depolarization-dependent inhibition of these channels must arise from another voltage-sensing mechanism. Here, we focus on the more strongly voltage-dependent gating in MthK that operates at depolarized voltages.

Voltage-dependent inhibition arises from a decrease in open times and increase in closed times with depolarization

To begin to constrain possible mechanisms underlying voltage-dependent inhibition of MthK, we measured the durations of channel openings and closings to determine their voltage sensitivity. We observed that in MthK channels, open times decreased and closed times increased with depolarization. To a first approximation, both mean open and mean closed times could be described with a single-exponential dependence on voltage (under the conditions in Fig. 1, D and E). The mean interval durations show some deviation from single-exponential

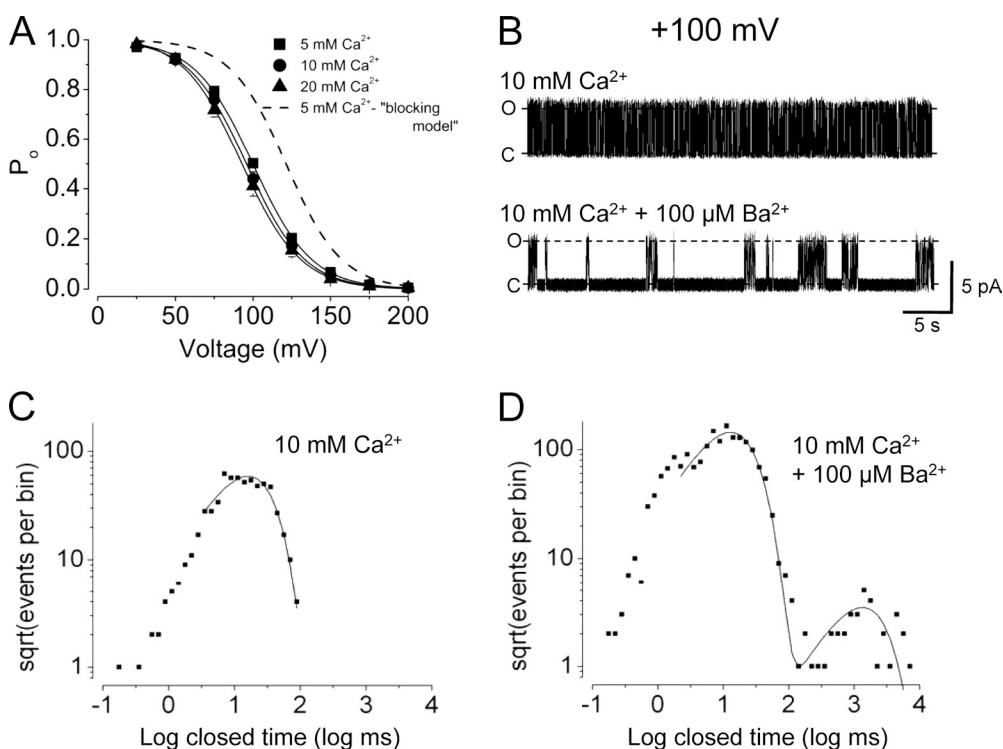


Figure 2. Inhibition of MthK at depolarized voltages is not because of Ca^{2+} or Ba^{2+} block from the cytoplasmic side. (A) Effects of decreasing $[Ca^{2+}]$ from 20 to 5 mM (filled symbols) are inconsistent with the predictions of a simple open-channel blocking model (dashed line). (B) Representative current in the absence and presence of added Ba^{2+} . 100 μ M Ba^{2+}_i resulted in an increase in long closings (presumed Ba^{2+} -blocking events). (C) Distribution of closed times in the absence of added Ba^{2+} . $V_m = 100$ mV. Closed times are described by a single exponential (solid line). (D) The addition of Ba^{2+} results in a second, kinetically distinct class of closed times, with a mean duration of ~ 1 s at 100 mV.

voltage dependence; these deviations arise in part from the lengthening of long-interval durations near 0 mV and near 200 mV because of missed brief events at these voltages, owing to the limited time resolution of the recordings. With both open and closed times, the deviations are reduced by applying a correction for missed events (Eq. 4; refer to Materials and methods). Fitting the corrected durations with single-exponential voltage dependence (Eq. 5) yielded an extrapolated mean open time at 0 mV of 310 ± 20 ms, which decreased with depolarization with an apparent gating valence of $-0.87 \pm 0.04 e_0$. Mean closed time extrapolated at 0 mV was 0.65 ± 0.08 ms and increased with depolarization with an apparent gating valence of $0.75 \pm 0.02 e_0$. This suggests that rates determining the lifetimes of both the opened and closed states entered at depolarized voltages, in aggregate, have approximately equal and oppositely charged gating valences. The means of the partial

charges estimated from the voltage dependence of mean open and closed times sum to an overall gating valence of $1.6 e_0$, consistent with the gating valence estimated from Boltzmann fits of P_o versus voltage relations (Fig. 1 C).

Voltage-dependent gating of MthK does not arise from slow ionic blockade

Because MthK activation requires millimolar concentrations of Ca^{2+} , and divalent cations may block K^+ channels with either slow or fast kinetics (Neyton and Miller, 1988a; Ferguson, 1991; Bello and Magleby, 1998), we initially hypothesized that the voltage-dependent gating of MthK may arise from slow ionic blockade of the channel by Ca^{2+} or, alternatively, Ba^{2+} , which is often present as a contaminant in Ca^{2+} - or K^+ -containing salt solutions.

To test the idea that Ca^{2+} might underlie MthK channel blockade, we examined the inhibition kinetics over

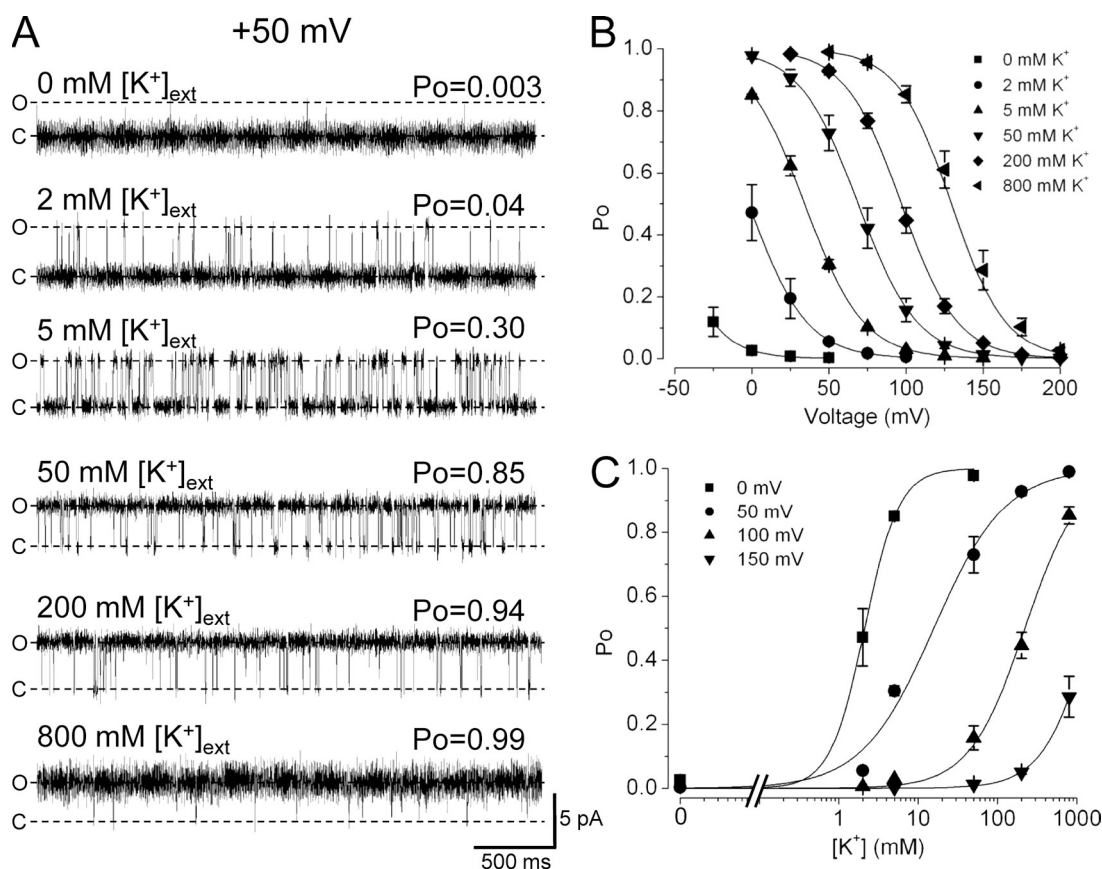
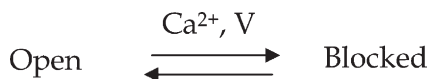


Figure 3. Increasing $[K^+]_{ext}$ stabilizes the open-conductive state at positive voltages. (A) Representative outward currents at 50 mV over a range of $[K^+]_{ext}$. (B) P_o versus V relations determined over a range of $[K^+]_{ext}$. These were each described by a Boltzmann equation (refer to Materials and methods; solid lines). Parameters were: 0 mM K^+ : $V_{1/2} = -56.3$ mV and $z\delta = 1.6$; 2 mM K^+ : $V_{1/2} = -2.1$ mV and $z\delta = 1.3$; 5 mM K^+ : $V_{1/2} = 34.2$ mV and $z\delta = 1.3$; 50 mM K^+ : $V_{1/2} = 68.9$ mV and $z\delta = 1.3$; 200 mM K^+ : $V_{1/2} = 96.9$ mV and $z\delta = 1.4$; 800 mM K^+ : $V_{1/2} = 129.4$ mV and $z\delta = 1.4$. Thus, increasing $[K^+]_{ext}$ from 0 to 800 mM shifts $V_{1/2}$ to more depolarized voltages, but does not systematically change the effective gating valence. (C) Mean P_o versus $[K^+]_{ext}$ at 0, 50, 100, and 150 mV. These were described by Hill equations (refer to Materials and methods; solid lines). Parameters were: 0 mV: $EC_{50} = 2.1$ mM and $n_H = 2.0$; 50 mV: $EC_{50} = 15$ mM and $n_H = 0.96$; 100 mV: $EC_{50} = 220$ mM and $n_H = 1.2$; 150 mV: $EC_{50} = 1,500$ mM and $n_H = 1.4$. These data suggest that open-state stabilization may be modulated by a single K^+ -binding site, and depolarization decreases the apparent affinity for K^+ .

a range of $[Ca^{2+}]$. In the context of a simple open-channel blocking model,



If inhibition were from a bimolecular interaction between Ca^{2+} and the channel, we predict that decreasing the $[Ca^{2+}]$ fourfold from 20 to 5 mM should increase mean open times fourfold and increase P_o (Fig. 2 A, dotted curve). In contrast, decreasing $[Ca^{2+}]$ over this range had nominal effects on P_o (Fig. 2 A, filled symbols and solid curves), inconsistent with Ca^{2+} blockade.

Likewise, if Ba^{2+} were the culprit, increasing $[Ba^{2+}]$ at the cytoplasmic side of the channel ($[Ba^{2+}]_{in}$) should proportionally increase the blocking rate. We observed, interestingly, that compared with mammalian large-conductance Ca^{2+} -activated K^+ channels, MthK has a relatively low sensitivity to slow blockade by internal Ba^{2+} (Miller et al., 1987; Neyton and Miller, 1988b; Bello and Magleby, 1998). However, raising $[Ba^{2+}]_{in}$ to 100 μM resulted in Ba^{2+} -blocking events that were clearly distinguishable from the voltage-dependent closings observed without Ba^{2+} (Fig. 2, B–D). Collectively, these observations suggest that the voltage-dependent gating of MthK is not because of slow ionic blockade, and may instead involve an intrinsic gating mechanism.

Voltage-dependent gating in MthK is sensitive to external K^+

If voltage-dependent gating is from an intrinsic mechanism, it might arise from a form of channel inactivation. A hallmark of C-type inactivation, as observed in Kv channels, is its sensitivity to $[K^+]_{ext}$ at the external side of the channel ($[K^+]_{ext}$); specifically, increasing $[K^+]_{ext}$ decreases the rate of inactivation at a given voltage, whereas decreasing $[K^+]_{ext}$ speeds it up (López-Barneo et al., 1993; Baukowitz and Yellen, 1995, 1996). We have observed a strikingly similar effect with MthK inactivation gating (Fig. 3). Decreasing $[K^+]_{ext}$ shifted gating leftward (i.e., less positive) on the voltage axis, effectively destabilizing the open-conductive state. Likewise, increasing $[K^+]_{ext}$ to 800 mM shifted closing, or “inactivation,” toward more positive voltages, effectively stabilizing the open-conductive state. Although $[K^+]_{ext}$ affected the $V_{1/2}$ of inactivation, it did not affect the effective gating valence ($z\delta$), consistent with the idea that voltage modulates the equilibrium among open-conductive and open-inactivated states, but not the number of charges underlying the gating process nor the interaction between these charges and the electric field.

To estimate the minimum number of K^+ ions involved in control of inactivation, we plotted P_o as a function of $[K^+]_{ext}$ at four different voltages (ranging from 0 to 150 mV) and fitted these data with a Hill equation (Eq. 3). We observed that the Hill coefficient did not change systematically over this voltage range, with a mean

Hill coefficient of 1.4 ± 0.2 (Fig. 3 C). Because the mean Hill coefficient was not significantly different from 1, these data are consistent either with a single K^+ being sufficient to stabilize the conductive state, or multiple K^+ ions acting either noncooperatively or with slight negative cooperativity to stabilize the conductive state. The results also illustrate that over voltages ranging from 0 to 150 mV, increasing depolarization increases the $[K^+]_{ext}$ required to suppress inactivation (ranging from 2.1 mM at 0 mV to 1.5 M at 150 mV), based on the data in Fig. 3 C. The basis for this apparent voltage dependence is not clear; possibilities include (a) directly voltage-driven K^+ binding to a site within the electric field; (b) voltage inducing (or facilitating) a conformational change that enhances K^+ binding; (c) voltage dependence arising from electrostatic coupling via the movement of K^+ ions through the selectivity filter; or (d) some combination of these possibilities.

Sensitivity of MthK voltage gating to external cations is selective for K^+ and Rb^+ over Na^+ and Li^+

If the external binding site for K^+ that modulates inactivation in MthK is located within the electric field, i.e., in the selectivity filter, one might expect external cation sensitivity of inactivation in this channel to display selectivity for K^+ over other monovalent cations such as Na^+ or Li^+ . To test this, we measured P_o over a range of voltages in the presence of different monovalent cations at the external side of the pore, substituted for K^+ (each at 200 mM; Fig. 4).

Based on the $V_{1/2}$ of steady-state inactivation in the presence of each cation, we observed that the ions tested displayed the selectivity sequence of $K^+ \approx Rb^+ > Cs^+ > Na^+ > Li^+ \approx NMG^+$. Although this sequence is qualitatively similar to the canonical selectivity sequence of K^+ -selective channels determined by permeability ratios, a K^+ -binding site within the selectivity filter might be expected to show even greater selectivity for K^+ over Rb^+ than what is observed, and an even greater still selectivity for K^+ over Na^+ (Coronado et al., 1980; Blatz and Magleby, 1984). One possible explanation for this could have been that the MthK selectivity filter may not be quite as K^+ selective as anticipated. However, in mixed-ion conditions (Fig. 4 B), both external K^+/Rb^+ and K^+/Na^+ solutions (100 mM of each ion) result in shifts in reversal potential consistent with “normal” K^+ -selective permeation properties (within the expected error limits) (LeMasurier et al., 2001). In addition, a recent analysis of ionic selectivity in MthK using slightly different mixed-ion conditions yielded a P_{Na}/P_K of 0.017, supporting the idea that in the presence of K^+ , the MthK permeation pathway is selective for K^+ over Na^+ (Ye et al., 2010). Collectively, these results are consistent with the idea that inactivation in MthK is modulated by a weakly selective ion-binding site, located toward the external side of the selectivity filter.

Voltage gating of MthK may be described by kinetic schemes in which the open-conductive state is stabilized by the binding of K^+

To describe the $[K^+]_{\text{ext}}$ and voltage dependence of Po at depolarized voltages, we developed a series of kinetic schemes in which both K^+ binding and hyperpolarization are coupled to relative energetic stabilization of the open-conductive state over the open-inactivated state. Rate constants and voltage dependences for transitions among conductive and inactivated states in the schemes were constrained by two-dimensional distributions of adjacent open and closed dwell-times obtained over a range of $[K^+]_{\text{ext}}$ and voltage for each channel (Rothberg and Magleby, 1998, 1999, 2000). Schemes were ranked statistically after applying a penalty for increasing the number of free parameters in a scheme, according to Eq. 6.

We took the approach of fitting the simplest scheme, with one open-conductive (O) and one open-inactivated (I) state, and then adding additional states (O or I) until a further addition yielded no significant improvement in the maximum likelihood value for the scheme. For each scheme, we also tested for the effects of different arrangements for transitions among O and I states, as well as different positions of the $[K^+]$ -dependent transition (defined by a second-order rate constant that scales with $[K^+]_{\text{ext}}$). All rate constants were assumed to have some exponential voltage dependence (Hodgkin and Huxley, 1952; Magleby and Stevens, 1972), with valences determined as fitted parameters constrained by the experimental data.

A series of schemes was tested by global fitting of data collected at three to four different $[K^+]_{\text{ext}}$ and three to

four different voltages at each $[K^+]_{\text{ext}}$, ranging from 0 to 200 mV (10–14 datasets per channel). Statistical ranking information for the top six ranked schemes (Fig. S1) is presented in Table S1. We observed that the schemes with the highest likelihoods share in common the property that the K^+ -dependent rate was positioned at an I→O transition; schemes in which the K^+ -dependent rate was placed at an I→I or O→O transition had lower likelihood values than otherwise equivalent schemes with the same numbers of O and I states. In the context of these schemes, this is consistent with the physical interpretation that once K^+ dissociates from its regulatory site near the external side of the channel, the channel undergoes a rapid transition to an I state. Each of the schemes also contains at least two I states connected by a voltage-dependent transition, consistent with at least two relatively stable nonconducting conformations, and an “intrinsic” voltage dependence driving the conformational change between these states. This voltage-dependence may arise from (a) ion movements within the selectivity filter that do not result in a net movement of K^+ through the filter, or (b) conformational changes in or near the pore that are independent of net K^+ flux.

Rate constants and effective partial charges associated with each gating transition, obtained from fitting with experimental data from three different single channels, are presented for Scheme 1 (Table I). Fitting and ranking of candidate schemes for three different single MthK channels suggested that Scheme 6 can best account for the major features of steady-state inactivation at depolarized voltages (Table S1); however, inspection of the rate constants obtained from fitting this scheme

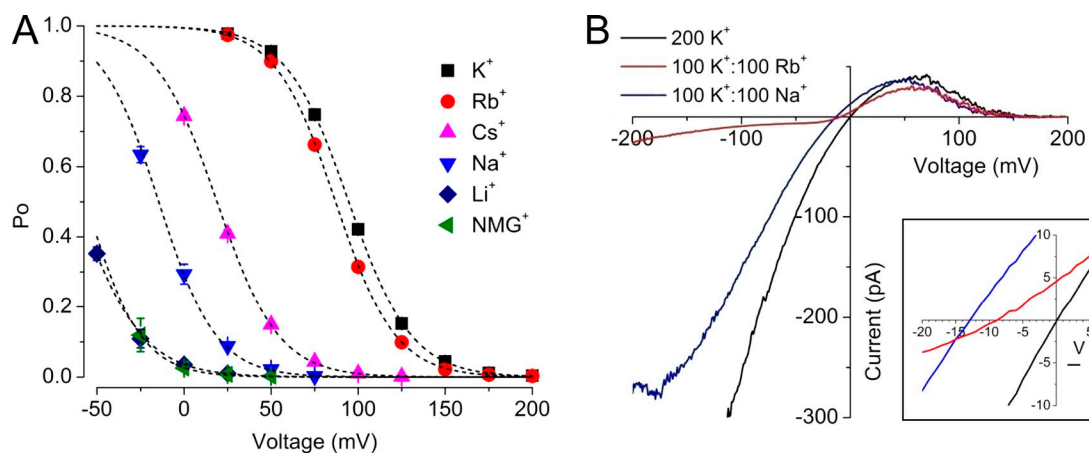


Figure 4. Ionic selectivity of an external modulatory site. (A) Po versus voltage with 200 mM of the indicated cation at the external side of the channel. Data were fitted with Boltzmann equations (dashed lines). Parameters were: K^+ : $V_{1/2} = 94.6$ mV and $z\delta = 1.4$; Rb^+ : $V_{1/2} = 87.0$ mV and $z\delta = 1.5$; Cs^+ : $V_{1/2} = 18.9$ mV and $z\delta = 1.4$; Na^+ : $V_{1/2} = -14.6$ mV and $z\delta = 1.5$; Li^+ : $V_{1/2} = -61.8$ mV and $z\delta = 1.3$; NMG^+ : $V_{1/2} = -56.3$ mV and $z\delta = 1.6$. Thus, Rb^+ was nearly as effective as K^+ at stabilizing the open-conductive state, followed by Cs^+ and Na^+ . Li^+ was the least effective, with nearly the same $V_{1/2}$ as NMG^+ . (B) Representative current–voltage relations assessed by voltage ramps from a bilayer containing ~ 10 MthK channels. Equimolar external K^+ and Rb^+ (100 mM each) resulted in a shift in reversal potential (V_{rev}) of around -9 mV, consistent with a moderate selectivity for K^+ over Rb^+ . Equimolar K^+/Na^+ yielded a shift of around -15 mV, which was the same as the shift observed for K^+/Li^+ (not depicted). Collectively, these results suggest that inactivation results from vacancy of an external cation-binding site that shows moderate K^+ selectivity.

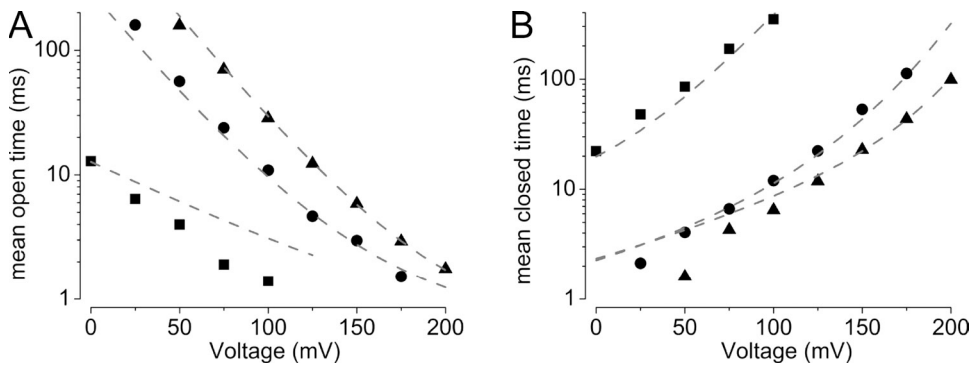
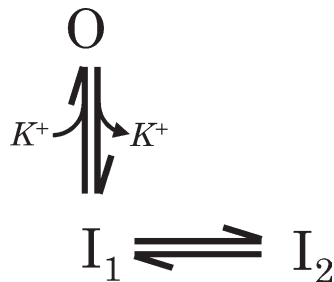


Figure 5. Predictions of a minimal kinetic scheme to describe the effects of $[K^+]_{\text{ext}}$ and voltage on MthK gating at depolarized voltages. (A) Mean open times from Channel 1 at 2, 200, and 800 mM K^+_{ext} plotted as a function of voltage (filled squares, circles, and triangles, respectively). Mean open times predicted using Scheme 1 with rate constants for Channel 1 are shown superimposed (Table 1; dashed gray). (B) Mean closed times from Channel 1 under the

same conditions, with predictions from Scheme 1 superimposed, as described in A. Collectively, these results are consistent with a gating mechanism that contains a minimum of one open-conductive (O) state and two open-inactivated (I) states, with the O state stabilized by weakly voltage-dependent K^+ binding.

using data from different channels suggests that rates for Scheme 6, with two O and three I states, can vary widely among channels (Table S2). In contrast, rates from Scheme 1 showed greater consistency among channels and are likely to be better constrained by the experimental data. Mean open and mean closed times predicted by Scheme 1 with the most likely rate constants for Channel 1 are presented superimposed on the experimental data (Fig. 5, dashed gray lines). Scheme 1 notably captures the basic voltage dependence of open and closed times over a 400-fold range of $[K^+]_{\text{ext}}$ from 2 to 800 mM, and at voltages ranging from 0 to 200 mV.



(SCHEME 1)

Limitations of Scheme 1

Although Scheme 1 describes the major features of MthK inactivation over a wide range of experimental conditions, this description is not ideal. Specifically, Scheme 1 predicts a too shallow voltage dependence of mean open time with 2 mM K^+_{ext} , and a too shallow voltage dependence of mean closed time with 800 mM K^+_{ext} . One possible explanation for the nonideal fits are that the K^+ -dependent transition rates were determined by scaling the second-order rate constants by $[K^+]$, which does not explicitly account for effects of ionic strength on K^+ activity. In our experiments, ionic strength was

kept constant at $[K^+]_{\text{ext}}$ ranging from 0 to 200 mM by substituting KCl with NMG^+ (with Cl^- as the counterion, added as HCl; refer to Materials and methods). However, solutions with 800 mM KCl had a slightly higher ionic strength, leading to an estimated 13.9% lower K^+ activity coefficient. By fitting kinetic schemes using an effective $[K^+]_{\text{ext}}$ of 688.8 mM for the 800-mM KCl dataset (refer to Materials and methods), we found that this decrease in activity coefficient had a nominal effect on maximum likelihood values and did not affect the rankings of the schemes. It is possible that incorporation of this kinetic scheme into the framework of the general model that accounts for other MthK-gating phenomena such as the Ca^{2+} and H^+ dependence, as well as the weak voltage-dependent gating at negative voltages, may provide a better description of these data (Zadek and Nimigean, 2006; Pau et al., 2010). For now, Scheme 1 should be considered a reasonable quantitative working hypothesis of MthK inactivation.

DISCUSSION

MthK inactivation is voltage dependent and sensitive

to $[K^+]_{\text{ext}}$

Our results show principally that MthK gating is modulated by a moderately voltage-dependent process at depolarized voltages that is linked to $[K^+]_{\text{ext}}$ (Figs. 1 and 3). Gating that is sensitive to $[K^+]_{\text{ext}}$ is reminiscent of C-type inactivation, a phenomenon that is common among Kv channels (Grissmer and Cahalan, 1989; Choi et al., 1991; Baukowitz and Yellen, 1995; Levy and Deutsch, 1996). Unlike Kv channels, however, MthK shows a relatively simple transmembrane architecture, with no canonical voltage sensor motif (Jiang et al., 2002). This eliminates any possible modulatory role of a voltage sensor in the gating process, and suggests that in the context of an otherwise open K^+ channel, this form of inactivation may arise from a conformational change at or near the K^+ selectivity filter, given a combination of permissive

structures around the filter. An understanding of the residues that determine this putative form of inactivation in MthK should provide further insight toward what now appears to be a general feature of K^+ channels (Cordero-Morales et al., 2006, 2007; Kurata et al., 2010).

Stabilization of the conductive state by ion occupancy at the external end of the pore

Our present results are consistent with the idea that in MthK, the open-conductive state is stabilized by K^+ binding to a site at the external end of the pore that shows moderate selectivity for K^+ over Na^+ , and an apparently strong selectivity for K^+ over Li^+ and NMG^+ (Fig. 4). Computational studies suggest that ion-binding sites at the internal and external ends of the KcsA selectivity filter (S0 and S4) are less selective than those deeper in the filter (S1, S2, and S3) (Noskov et al., 2004). In addition, high-resolution x-ray crystallographic data from the MthK pore in the presence of Na^+ is consistent with a Na^+ ion binding in the plane of the carbonyl oxygens of Tyr62 at the external end of the selectivity filter (Ye et al., 2010). Because K^+ binding at a site equivalent to the S0 site of KcsA is not observed in the high-resolution MthK pore structure, the available data are (to a first approximation) consistent with the idea that K^+ binding in the S1 “cage” formed by the carbonyl oxygens of Gly61 and Tyr62 may act to stabilize the conductive state; this stabilization may also be achieved by Na^+ binding in the plane formed by the carbonyl oxygens of Tyr62.

Physical interpretation of Scheme 1

We propose a relatively simple kinetic scheme, Scheme 1, to account for the major features of voltage-dependent gating in MthK over a wide range of depolarized voltages and $[K^+]_{ext}$, although it is presumed that this scheme is a simplification of the actual gating mechanism. In the context of this scheme, open-conductive channels undergo a moderately voltage-dependent transition to an open-inactivated (I) state ($z\delta \approx 0.5$), concurrent with dissociation of K^+ , whereas the transition to the open-conductive (O) state, which accompanies K^+ binding, is governed by a fast second-order rate constant (4 to $5 \times 10^4 M^{-1} s^{-1}$) and has a relatively weak voltage dependence ($z\delta \leq -0.1$). These rate constants and voltage dependences

are consistent with the idea that external K^+ binds to a selectivity filter site that is located only a short distance across the transmembrane electric field, and K^+ binding over a wide range of voltages is rapid and may approach the diffusion limit. In contrast, K^+ dissociation is more strongly voltage dependent, which could be attributed either to (a) coupled movement of K^+ through the pore (i.e., knockoff of K^+ from the binding site because of outward movement of K^+) or (b) a voltage-dependent conformational change that would increase K^+ dissociation with increasing depolarization. Experimental support for both of these possibilities exists in Kv channels, but structural determinants of inactivation in Shaker K^+ channels may be different from those in MthK, so the nature of a possible conformational change in this gating process is unclear (Baukrowitz and Yellen, 1996; Liu et al., 1996).

In addition to the central voltage and K^+ -dependent transition, Scheme 1 involves at least one other transition among inactivated states that does not involve a net association/dissociation of K^+ from the channels. This could involve ion movements within the selectivity filter (i.e., translocation of ions among different binding sites) and may be coupled to a conformational change in the channel.

Relation between inactivation phenomena observed in MthK and KcsA and corresponding structural observations
Crystallographic experiments reveal that at low permeant ion concentrations, the KcsA channel assumes a “collapsed” conformation, which involves a structural rearrangement in the backbone at the channel’s selectivity filter, as well as rearrangements in ion occupancy at the K^+ -binding sites (Zhou et al., 2001; Zhou and MacKinnon, 2004). The existence of high- K^+ “conductive” and low- K^+ “collapsed” conformations of the KcsA selectivity filter, combined with functional observations that KcsA channels can inactivate after a jump in $[H^+]$, suggests that the collapsed filter may provide a physical explanation for inactivation (Cordero-Morales et al., 2006, 2007). Recently, an N-terminal truncated form of KcsA was crystallized in the collapsed conformation despite the presence of high K^+ , providing further evidence that the collapsed filter may underlie an open-inactivated state (Cuello et al., 2010).

TABLE I
Rate constants for Scheme 1

Transition	Channel 1		Channel 2		Channel 3	
	Rate constant s^{-1}	Partial charge e_0	Rate constant s^{-1}	Partial charge e_0	Rate constant s^{-1}	Partial charge e_0
$k_{O,I1}$	86	0.39	32	0.53	31	0.57
$k_{I1,O}$	$50,000 M^{-1}$	-0.11	$48,000 M^{-1}$	-0.11	$37,000 M^{-1}$	-0.03
$k_{I1,I2}$	450	0.45	410	0.47	1,100	0.29
$k_{I2,I1}$	570	-0.36	480	-0.30	530	-0.34

If the collapsed KcsA filter represents an open-inactivated conformation, our observation of inactivation in MthK with similar properties suggests that a similar collapsed structure might be observed with the MthK pore in low K^+ , but surprisingly this has not been the case (Ye et al., 2010). Although the MthK selectivity filter shows clear changes in ion occupancy in low K^+ , a collapse of the MthK selectivity filter has not been observed.

Is it possible that the low K^+ , noncollapsed MthK pore is not in the inactivated state? If we assume that the MthK pore structures represent conformations at 0 mV, we would expect them to be in the inactivated state if external K^+ were replaced with Li^+ or NMG^+ , or, to a lesser extent, Na^+ . Such side-specific ion substitutions are not possible within a crystal; consequently, these structures represent conformations under mixed-ion conditions for which detailed functional data are not yet available. In addition, Na^+ is not completely inept at stabilizing the open-conductive state of MthK at 0 mV (Fig. 4), although it is around 100-fold less effective than K^+ in terms of external ionic concentration (Fig. 3). Thus, the possibility that the MthK pore structure in high Na^+ and low or 0 K^+ is in an open-conductive state has not been ruled out.

Alternatively, it is possible that changes in K^+ occupancy within the selectivity filter, most notably the low K^+ occupancy of the S2 site and/or reduced occupancy of the S4 site in the low K^+ MthK pore structures (also observed in the collapsed KcsA structures), may themselves yield a nonconducting state, and that pore collapse is not an obligatory component of inactivation. Vacancy of the S2 site has been hypothesized as a mechanism underlying an asymmetrical conformational change in the KcsA selectivity filter, based on molecular dynamics simulations, which would be difficult to resolve in an x-ray structure (Bernèche and Roux, 2005). It is also possible that inactivation in MthK and KcsA are heterogeneous processes with different underlying mechanisms, despite the similarities in their properties.

So why doesn't the MthK filter collapse in crystallographic conditions that yield filter collapse in KcsA? As suggested above, one possibility is that multiple Na^+ ions are capable of stabilizing the MthK selectivity filter and may prevent pore collapse, whereas they are unable to stabilize the KcsA selectivity filter. It has been observed that the KcsA pore can be stabilized in the noncollapsed form in the presence of Li^+ , even in low K^+ , consistent with the idea that some impermeant ions can act as countercharges within the filter to prevent electrostatic repulsion of the backbone carbonyl oxygens (and filter collapse) (Thompson et al., 2009).

Possible role of a hydrogen bond network in the pore helix
In KcsA, inactivation seems to depend on a hydrogen bond network that involves water coordination between a highly conserved aspartate residue, Asp80, and the

pore helix residue Glu71 (Cordero-Morales et al., 2006, 2007). When water coordination is perturbed by the mutation E71A, inactivation in KcsA is effectively abolished, although the physical mechanism underlying this effect is unclear. Although the MthK residue analogous to Glu71, Val55, is hydrophobic and thus does not directly participate in hydrogen bonding, the MthK residue analogous to Asp80 (Asp64 in MthK) is involved in a hydrogen-bonding network, yielding a structure similar to wild-type KcsA (Ye et al., 2010). This is consistent with the idea that these hydrogen bond networks are somehow critical to inactivation in each of these channels. It will be important to further understand the properties of these structures that modulate transitions to the inactivated state.

We thank Victor Pau and Karin Abarca-Heidemann for helpful discussions.

This work was supported by grants from the National Institutes of Health (grant R01 GM068523) and the Pennsylvania Department of Health.

Lawrence G. Palmer served as editor.

Submitted: 29 July 2010

Accepted: 27 September 2010

REFERENCES

- Baukrowitz, T., and G. Yellen. 1995. Modulation of K^+ current by frequency and external $[K^+]$: a tale of two inactivation mechanisms. *Neuron*. 15:951–960. doi:10.1016/0896-6273(95)90185-X
- Baukrowitz, T., and G. Yellen. 1996. Use-dependent blockers and exit rate of the last ion from the multi-ion pore of a K^+ channel. *Science*. 271:653–656. doi:10.1126/science.271.5249.653
- Bello, R.A., and K.L. Magleby. 1998. Time-irreversible subconductance gating associated with Ba^{2+} block of large conductance Ca^{2+} -activated K^+ channels. *J. Gen. Physiol.* 111:343–362. doi:10.1085/jgp.111.2.343
- Bernèche, S., and B. Roux. 2005. A gate in the selectivity filter of potassium channels. *Structure*. 13:591–600. doi:10.1016/j.str.2004.12.019
- Blatz, A.L., and K.L. Magleby. 1984. Ion conductance and selectivity of single calcium-activated potassium channels in cultured rat muscle. *J. Gen. Physiol.* 84:1–23. doi:10.1085/jgp.84.1.1
- Blatz, A.L., and K.L. Magleby. 1986. Correcting single channel data for missed events. *Biophys. J.* 49:967–980. doi:10.1016/S0006-3495(86)83725-0
- Brugada, R., K. Hong, R. Dumaine, J. Cordeiro, F. Gaita, M. Borggrefe, T.M. Menendez, J. Brugada, G.D. Pollevick, C. Wolpert, et al. 2004. Sudden death associated with short-QT syndrome linked to mutations in HERG. *Circulation*. 109:30–35. doi:10.1161/01.CIR.0000109482.92774.3A
- Choi, K.L., R.W. Aldrich, and G. Yellen. 1991. Tetraethylammonium blockade distinguishes two inactivation mechanisms in voltage-activated K^+ channels. *Proc. Natl. Acad. Sci. USA*. 88:5092–5095. doi:10.1073/pnas.88.12.5092
- Cordeiro, J.M., R. Brugada, Y.S. Wu, K. Hong, and R. Dumaine. 2005. Modulation of I(Kr) inactivation by mutation N588K in KCNH2: a link to arrhythmogenesis in short QT syndrome. *Cardiovasc. Res.* 67:498–509. doi:10.1016/j.cardiores.2005.02.018
- Cordero-Morales, J.F., L.G. Cuello, Y. Zhao, V. Jogini, D.M. Cortes, B. Roux, and E. Perozo. 2006. Molecular determinants of gating at the potassium-channel selectivity filter. *Nat. Struct. Mol. Biol.* 13:311–318. doi:10.1038/nsmb1069

- Cordero-Morales, J.F., V. Jogini, A. Lewis, V. Vásquez, D.M. Cortes, B. Roux, and E. Perozo. 2007. Molecular driving forces determining potassium channel slow inactivation. *Nat. Struct. Mol. Biol.* 14:1062–1069. doi:10.1038/nsmb1309
- Coronado, R., R.L. Rosenberg, and C. Miller. 1980. Ionic selectivity, saturation, and block in a K⁺-selective channel from sarcoplasmic reticulum. *J. Gen. Physiol.* 76:425–446. doi:10.1085/jgp.76.4.425
- Cuello, L.G., V. Jogini, D.M. Cortes, and E. Perozo. 2010. Structural mechanism of C-type inactivation in K(+) channels. *Nature.* 466:203–208. doi:10.1038/nature09153
- Ferguson, W.B. 1991. Competitive Mg²⁺ block of a large-conductance, Ca²⁺-activated K⁺ channel in rat skeletal muscle. Ca²⁺, Sr²⁺, and Ni²⁺ also block. *J. Gen. Physiol.* 98:163–181. doi:10.1085/jgp.98.1.163
- Grissmer, S., and M. Cahalan. 1989. TEA prevents inactivation while blocking open K⁺ channels in human T lymphocytes. *Biophys. J.* 55:203–206. doi:10.1016/S0006-3495(89)82793-6
- Hille, B. 2001. *Ion Channels of Excitable Membranes*. Third edition. Sinauer Associates, Sunderland, MA. 814 pp.
- Hodgkin, A.L., and A.F. Huxley. 1952. A quantitative description of membrane current and its application to conduction and excitation in nerve. *J. Physiol.* 117:500–544.
- Hoshi, T., W.N. Zagotta, and R.W. Aldrich. 1991. Two types of inactivation in Shaker K⁺ channels: effects of alterations in the carboxy-terminal region. *Neuron.* 7:547–556. doi:10.1016/0896-6273(91)90367-9
- Jiang, Y., A. Lee, J. Chen, M. Cadene, B.T. Chait, and R. MacKinnon. 2002. Crystal structure and mechanism of a calcium-gated potassium channel. *Nature.* 417:515–522. doi:10.1038/417515a
- Kaye, G.W.C., and T.H. Laby. 1995. *Tables of Physical and Chemical Constants*. 16th edition. Longman, Essex/New York. 611 pp.
- Kurata, H.T., M. Rapedius, M.J. Kleinman, T. Baukrowitz, and C.G. Nichols. 2010. Voltage-dependent gating in a “voltage sensor-less” ion channel. *PLoS Biol.* 8:e1000315. doi:10.1371/journal.pbio.1000315
- LeMasurier, M., L. Heginbotham, and C. Miller. 2001. KcsA: it’s a potassium channel. *J. Gen. Physiol.* 118:303–314. doi:10.1085/jgp.118.3.303
- Levy, D.I., and C. Deutsch. 1996. Recovery from C-type inactivation is modulated by extracellular potassium. *Biophys. J.* 70:798–805. doi:10.1016/S0006-3495(96)79619-4
- Liu, Y., M.E. Jurman, and G. Yellen. 1996. Dynamic rearrangement of the outer mouth of a K⁺ channel during gating. *Neuron.* 16:859–867. doi:10.1016/S0896-6273(00)80106-3
- Loots, E., and E.Y. Isacoff. 2000. Molecular coupling of S4 to a K⁺ channel’s slow inactivation gate. *J. Gen. Physiol.* 116:623–636. doi:10.1085/jgp.116.5.623
- López-Barneo, J., T. Hoshi, S.H. Heinemann, and R.W. Aldrich. 1993. Effects of external cations and mutations in the pore region on C-type inactivation of Shaker potassium channels. *Receptors Channels.* 1:61–71.
- Magleby, K.L. 1992. Ion channels. Preventing artifacts and reducing errors in single-channel analysis. *Methods Enzymol.* 207:763–791. doi:10.1016/0076-6879(92)07055-S
- Magleby, K.L., and C.F. Stevens. 1972. The effect of voltage on the time course of end-plate currents. *J. Physiol.* 223:151–171.
- Magleby, K.L., and D.S. Weiss. 1990. Estimating kinetic parameters for single channels with simulation. A general method that resolves the missed event problem and accounts for noise. *Biophys. J.* 58:1411–1426. doi:10.1016/S0006-3495(90)82487-5
- McManus, O.B., and K.L. Magleby. 1991. Accounting for the Ca(2+)-dependent kinetics of single large-conductance Ca(2+)-activated K⁺ channels in rat skeletal muscle. *J. Physiol.* 443:739–777.
- McPate, M.J., R.S. Duncan, J.T. Milnes, H.J. Witchel, and J.C. Hancox. 2005. The N588K-HERG K⁺ channel mutation in the ‘short QT syndrome’: mechanism of gain-in-function determined at 37 degrees C. *Biochem. Biophys. Res. Commun.* 334:441–449. doi:10.1016/j.bbrc.2005.06.112
- Miller, C., R. Latorre, and I. Reisin. 1987. Coupling of voltage-dependent gating and Ba²⁺ block in the high-conductance, Ca²⁺-activated K⁺ channel. *J. Gen. Physiol.* 90:427–449. doi:10.1085/jgp.90.3.427
- Neyton, J., and C. Miller. 1988a. Discrete Ba²⁺ block as a probe of ion occupancy and pore structure in the high-conductance Ca²⁺-activated K⁺ channel. *J. Gen. Physiol.* 92:569–586. doi:10.1085/jgp.92.5.569
- Neyton, J., and C. Miller. 1988b. Potassium blocks barium permeation through a calcium-activated potassium channel. *J. Gen. Physiol.* 92:549–567. doi:10.1085/jgp.92.5.549
- Noskov, S.Y., S. Bernèche, and B. Roux. 2004. Control of ion selectivity in potassium channels by electrostatic and dynamic properties of carbonyl ligands. *Nature.* 431:830–834. doi:10.1038/nature02943
- Parfenova, L.V., B.M. Crane, and B.S. Rothberg. 2006. Modulation of MthK potassium channel activity at the intracellular entrance to the pore. *J. Biol. Chem.* 281:21131–21138. doi:10.1074/jbc.M603109200
- Pau, V.P., K. Abarca-Heidemann, and B.S. Rothberg. 2010. Allosteric mechanism of Ca²⁺ activation and H⁺-inhibited gating of the MthK⁺ channel. *J. Gen. Physiol.* 135:509–526. doi:10.1085/jgp.200910387
- Rothberg, B.S., and K.L. Magleby. 1998. Kinetic structure of large-conductance Ca²⁺-activated K⁺ channels suggests that the gating includes transitions through intermediate or secondary states. A mechanism for flickers. *J. Gen. Physiol.* 111:751–780. doi:10.1085/jgp.111.6.751
- Rothberg, B.S., and K.L. Magleby. 1999. Gating kinetics of single large-conductance Ca²⁺-activated K⁺ channels in high Ca²⁺ suggest a two-tiered allosteric gating mechanism. *J. Gen. Physiol.* 114:93–124. doi:10.1085/jgp.114.1.93
- Rothberg, B.S., and K.L. Magleby. 2000. Voltage and Ca²⁺ activation of single large-conductance Ca²⁺-activated K⁺ channels described by a two-tiered allosteric gating mechanism. *J. Gen. Physiol.* 116:75–99. doi:10.1085/jgp.116.1.75
- Rothberg, B.S., R.A. Bello, and K.L. Magleby. 1997. Two-dimensional components and hidden dependencies provide insight into ion channel gating mechanisms. *Biophys. J.* 72:2524–2544. doi:10.1016/S0006-3495(97)78897-0
- Schwarz, G. 1978. Estimating the dimension of a model. *Ann. Stat.* 6:461–464. doi:10.1214/aos/1176344136
- Smith, P.L., and G. Yellen. 2002. Fast and slow voltage sensor movements in HERG potassium channels. *J. Gen. Physiol.* 119:275–293. doi:10.1085/jgp.119.3.275
- Smith, P.L., T. Baukrowitz, and G. Yellen. 1996. The inward rectification mechanism of the HERG cardiac potassium channel. *Nature.* 379:833–836. doi:10.1038/379833a0
- Thompson, A.N., I. Kim, T.D. Panosian, T.M. Iverson, T.W. Allen, and C.M. Nimigean. 2009. Mechanism of potassium-channel selectivity revealed by Na(+) and Li(+) binding sites within the KcsA pore. *Nat. Struct. Mol. Biol.* 16:1317–1324. doi:10.1038/nsmb.1703
- Ye, S., Y. Li, and Y. Jiang. 2010. Novel insights into K⁺ selectivity from high-resolution structures of an open K⁺ channel pore. *Nat. Struct. Mol. Biol.* 17:1019–1023. doi:10.1038/nsmb.1865
- Yellen, G. 1998. The moving parts of voltage-gated ion channels. *Q. Rev. Biophys.* 31:239–295. doi:10.1017/S0033583598003448
- Yellen, G., D. Sodickson, T.Y. Chen, and M.E. Jurman. 1994. An engineered cysteine in the external mouth of a K⁺ channel allows inactivation to be modulated by metal binding. *Biophys. J.* 66:1068–1075. doi:10.1016/S0006-3495(94)80888-4
- Zadek, B., and C.M. Nimigean. 2006. Calcium-dependent gating of MthK, a prokaryotic potassium channel. *J. Gen. Physiol.* 127:673–685. doi:10.1085/jgp.200609534
- Zhou, Y., and R. MacKinnon. 2004. Ion binding affinity in the cavity of the KcsA potassium channel. *Biochemistry.* 43:4978–4982. doi:10.1021/bi049876z
- Zhou, Y., J.H. Morais-Cabral, A. Kaufman, and R. MacKinnon. 2001. Chemistry of ion coordination and hydration revealed by a K⁺ channel-Fab complex at 2.0 Å resolution. *Nature.* 414:43–48. doi:10.1038/35102009